



Original Research Article

Green and Eco-Friendly Synthesis of 2-Amino-3-Cyano-4*H*-Chromene Derivatives via Eggshell/Fe₃O₄ as a Biodegradable Polymer Matrix Nanocomposite

Hossein Ghafuri* , Mahsan Zargari, Atefeh Emami 

Catalysts and Organic Synthesis Research Laboratory, Department of Chemistry, Iran University of Science and Technology, Tehran 16846-13114, Iran

ARTICLE INFORMATION

Received: 15 January 2023
Received in revised: 9 February 2023
Accepted: 21 February 2023
Available online: 10 March 2023

DOI: 10.22034/ajgc.2023.1.7

KEYWORDS

Eggshell/Fe₃O₄
4*H*-Chromene
Polymer nanocomposite
Reusability

ABSTRACT

In this study, Eggshell/Fe₃O₄, a new biodegradable nanocomposite from natural source compounds, was synthesized and utilized to synthesize 2-amino-3-cyano-(4*H*)-chromene derivatives via green and eco-friendly conditions. The characterization of nanocomposite was done by Fourier Transform Infrared Spectroscopy (FT-IR), Scanning Electron Microscopy (SEM), X-ray Diffraction (XRD), Thermal Gravimetric Analysis (TGA), and Vibrating Sample Magnetometer (VSM). The green and biodegradable catalyst, easy recovery, reusability of catalyst, and simple workup with quantitative yields are considerable advantages of this method.

© 2023 by SPC (Sami Publishing Company), Asian Journal of Green Chemistry, Reproduction is permitted for noncommercial purposes.

Graphical Abstract



Introduction

In recent years, attention has been concentrated on eco-friendly and economically sustainable procedures synthesizing organic compounds. Likewise, the attempts to progress the solvent-free methods with short reaction times, high-yield products, and economic conditions were promoted [1-4]. Nowadays, the use of natural source catalysts is of high significance. Eggshell wastes are abundant and cheap biomaterials, which mainly consisting of calcium carbonate (main principle), acid amines, uronic acid, proteins, carbohydrates, and lipids. Concerning this interesting ingredient, eggshell can be considered a green catalyst in some organic syntheses which need a base catalyst [5-8]. On the other side, magnetic nanoparticles have recently been widely used in some new important chemical reactions like drug delivery, magnetic resonance imaging, hyperthermia cancer treatment, and bio-separation [9-12].

Generally, a composite combines two or more materials containing matrix and fillers. Nanocomposites consist of materials with one or more phases with nanoscale dimensions. The properties of nanocomposites are related to different factors such as size, shape, constituent phases, relative amounts, loading and distribution of the dispersed phase as well as interactions between the matrix and the dispersed phase [13-16]. In this research, to improve the magnetic properties of synthesized nanocomposite (Eggshell/Fe₃O₄), we used Fe₃O₄ as an important nanoparticle in the matrix of Eggshell. Furthermore, Fe₃O₄ nanoparticles can be improved the mechanical properties of this new nanocomposite. Regarding this consideration, ES/Fe₃O₄ can be an excellent biocatalyst in synthesizing some organic compounds. 2-Amino-chromenes are from the significant class of organic compounds with the main components of natural products. They are used as pigments, cosmetics, and biodegradable agrochemicals [17-21]. In addition, they have

interesting biological activities such as anti-cancer, antimicrobial, antioxidant, and antiproliferative properties. Moreover, they have other applications like potential calcium channel antagonists, anti-inflammatory agents, antiviral, diuretic, anti-coagulant, spasmolytic, anti-anaphylactic, and anti-HIV agents [22-24]. Moreover, they are used to treat neurodegenerative diseases involving Parkinson's disease, down's syndrome, Alzheimer's disease, Huntington's disease, Down syndrome, analgesics, and myorelaxant [25-28]. Due to the applications mentioned above and the importance of these compounds, versatile methods under different conditions have been reported to synthesize 2-amino-3-cyano-4*H*-Chromenes. One of the most common of these methods is different using catalysts including metal oxides (such as ZnO), chemical indicators (such as NaOH), organic bases, and ionic liquids by condensation of aldehyde, malononitrile, and 1, 3-dicarbonyl compounds [29-31]. Despite all attempts, this procedure is safer from several disadvantages, including expensive catalysts, harsh reaction conditions, tedious workup and fewer yields, long reaction time, and hazardous solvent. There is still broad scope to make efficient, economically viable, and eco-friendly methods for synthesizing 2-amino-3-cyano-4*H*-Chromenes. In this study, 2-amino-3-cyano-4*H*-Chromenes was synthesized via Eggshell/Fe₃O₄ as an efficient and new biocomposite under mild conditions. This method has outstanding advantages, such as using a green and biodegradable catalyst, easy recovery, reusability of catalyst, and simple workup with quantitative yields. The main text of the article should appear here with headings as appropriate.

Experimental

Materials and methods

All materials were obtained in the standard laboratory via standard techniques (unless else noted). All solvents, reagents, and chemicals were purchased from Merck and Aldrich without further purification. Reactions and products were studied and characterized by standard techniques. IR spectra were done on a Shimadzu IR-470 spectrometer, NMR spectra were taken on a Bruker DRX-500 Avance spectrometer, XRD measurements were taken on an X Pert MPD (40 kV, 40 mA), TGA was taken on NETZSCH TG 209, FE-SEM images were taken on a Sigma Zeiss and melting points were taken on an Electrothermal 9100 apparatus. All compounds were isolated by crystallization.

Preparation of magnetic eggshells nanocomposite

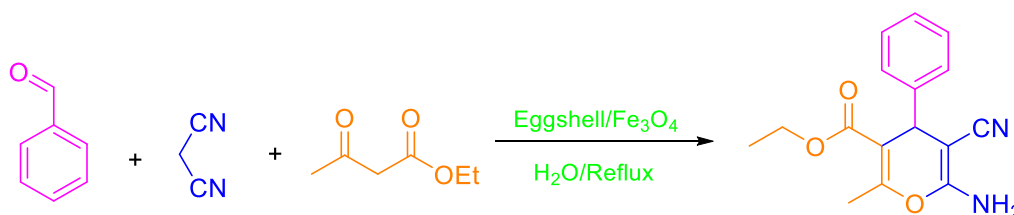
1.0 g Eggshells were initially collected and boiled in 0.5 mol/L NaOH solution for 1 h, washed several times with deionized water, and dried at 80 °C in oven for 24 h. To produce magnetic nanoparticles, a coprecipitation method was applied. A mixture of FeCl₃·6H₂O (12.2 g) and FeCl₂·4H₂O (4.7 g) in 50 mL of H₂O was prepared. Then, 1.5 mol/L NaOH solution was added dropwise at 60 °C under an N₂ atmosphere and stirred for 1 h. Afterward, the reaction temperature was increased to 80 °C and stirred for another 1 h. Finally, the prepared Eggshell/Fe₃O₄ was washed with deionized water and dried under vacuum for 12 h [14].

Synthesis of 2-amino-3-cyano-(4H)-pyrans

The solution of benzaldehyde (0.1 g), malononitrile (0.66 g), ethyl acetoacetate (0.13 g), Eggshell/Fe₃O₄ (0.03 g), and H₂O (3 mL) was mixed under reflux conditions. After the completion of the reaction (monitored by TLC (*n*-hexane, EtOAc, 3:1)), the intended products were obtained by simple recrystallization.

Results and Discussion

To achieve the most optimized ratio, Eggshell/ Fe_3O_4 nanocomposites were prepared in different concentrations of Eggshell to Fe_3O_4 . Finally, the best ratio of Eggshell and Fe_3O_4 was determined (Table 1, entry 2). In the following, to study the catalytic performance of the prepared nanocomposite, three-component reaction of benzaldehyde, malononitrile, and ethyl acetoacetate was considered as a model reaction (Scheme 1). (Eggshell/ Fe_3O_4 :5/1) was used in the synthesis of chromene derivatives.



Scheme 1. Optimization the ratio of Eggshell- Fe_3O_4 in model reaction.

Table 1. Different ratios between Eggshell and Fe_3O_4

Entry	Ratio (Eggshell: Fe_3O_4)	Time(min)	Yield (%) ^a
1	1:1	120	51
2	5:1	10	96
3	0.5:1	Just intermediate is formed	-
4	4:1	60	74

^a Isolated yield

Table 2. Different types of catalysts

Entry	Catalyst	Time (min)	Yield (%) ^a
1	ES/ Fe_3O_4	10	96
2	ES	180	90
3	ES+ Fe_3O_4	180	85
4	Fe_3O_4	240	60

^a Isolated yield

FT-IR spectra analysis

The FT-IR spectra of ES/ Fe_3O_4 MNPS nanocomposite are demonstrated in Figure 1. According to FT-IR analysis, the peaks at 2505 cm^{-1} (HCO_3), 1795 cm^{-1} (CO), 1421 cm^{-1} (C-O), 876 cm^{-1} (O-C-O), and 709 cm^{-1} (C-O) are related to carbonate absorptions. The adsorption band at 588 cm^{-1} is ascribed to stretching vibration

Calcium carbonate is the main component of Eggshell, which causes an alkaline media, and the Fe_3O_4 preparation has been done without using more external bases.

Different components were used separately in the model reaction to determine each component's effect, and the results were summarized in Table 1. As shown in Table 1, the product was formed in the presence of Eggshell/ Fe_3O_4 with the highest yield and the lowest time. Furthermore, the different types of applied catalysts are presented in Table 2.

(Fe-O-Fe), and the broad band at 3414 cm^{-1} is attributed to the OH stretching vibration in $\text{Ca}(\text{OH})_2$ (probably due to the adsorption of water on the surface of the magnetic nanocomposite) [32, 33].

Thermal gravimetric analysis (TGA)

TGA and DTG investigated the Eggshell/ Fe_3O_4 magnetic nanocomposite's thermal

stability at room temperature to 900 °C. As depicted in Figure 2, it was appointed that the weight loss less than 600 °C is attributed to the adsorbed water. The main decrease of weight ascribed to the decomposition of the Eggshell to CaO and CO₂ confirms the existence of the carbonate in the eggshell structure.

Field emission scanning electron microscopy (FE-SEM)

According to Figure 3, the Eggshell surface is completely covered by the magnetic Fe₃O₄ with spherical morphology. In addition, the FE-SEM images indicate that the average diameter of Fe₃O₄ is about 76 nm. Regarding the images, well distribution of Fe₃O₄ on the porous surface of the Eggshell, this nanocomposite has a huge surface area.

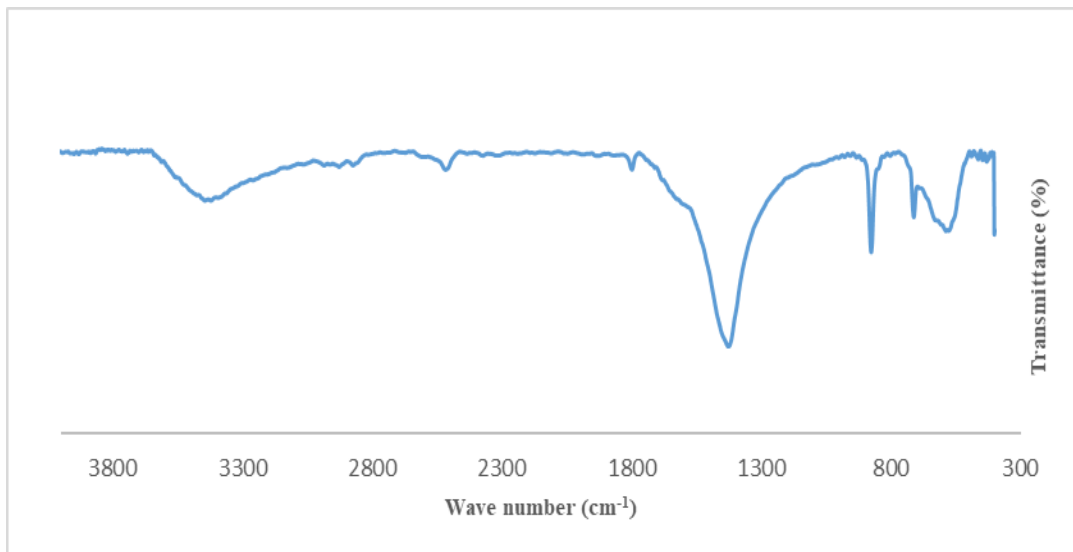


Figure 1. IR adsorption spectra of ES/ Fe₃O₄ MNPS nanocomposite

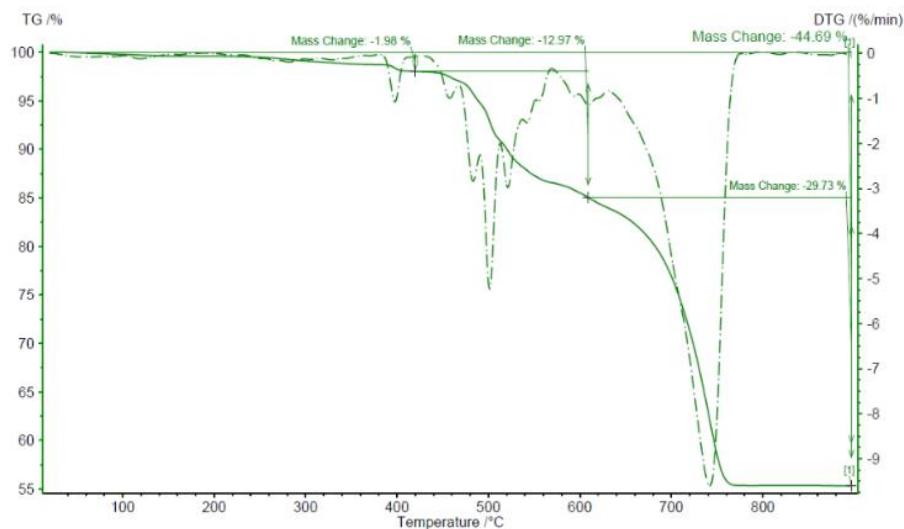


Figure 2. TGA curve of mass change ES/Fe₃O₄ MNPs.

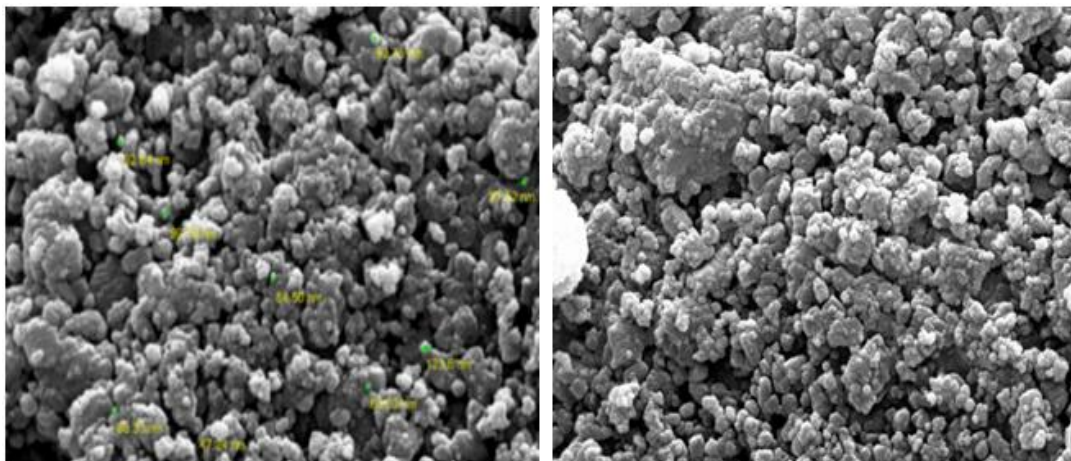


Figure 3. The FE-SEM images of ES/Fe₃O₄ nanocomposite

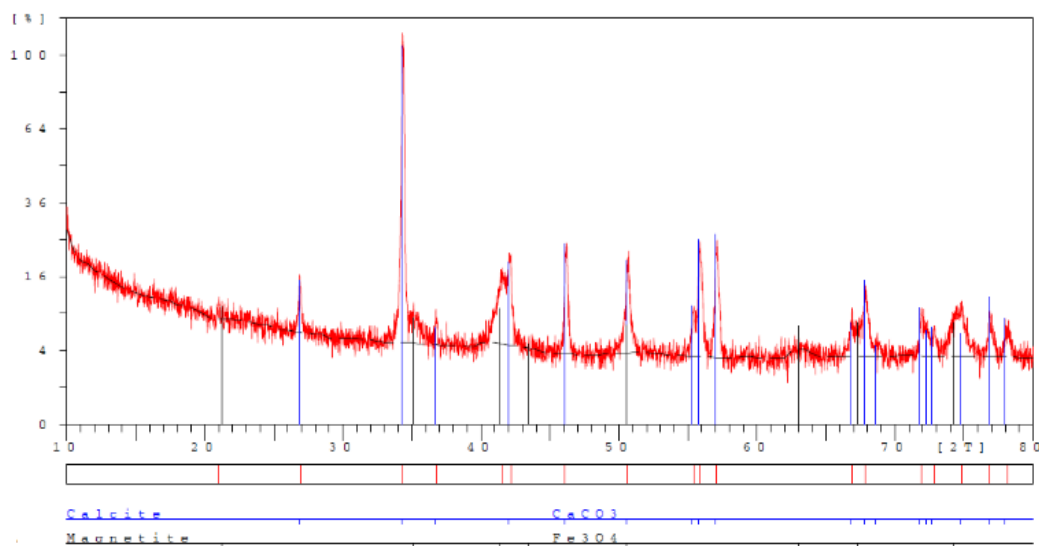


Figure 4. The XRD pattern of magnetic ES/Fe₃O₄

X-ray diffraction analysis (XRD)

As shown in the XRD patterns, the main peak at $2\theta = 34^\circ$ ascribed to the phase of eggshell (Figure 4). The peaks at $2\theta = 21^\circ, 36^\circ, 41^\circ, 43^\circ, 51^\circ, 63^\circ, 67^\circ,$ and 74° are attributed to the Fe₃O₄ phase (JCPD files no.98-0073). These data confirm the existence of CaCO₃ (JCPD 5-0586) in the eggshell structure and the presence of Fe₃O₄ in the nanocomposite structure. According to the results of the method reaction, the best ratio of Eggshell and Fe₃O₄ was determined to

prepare the optimized catalyst (Eggshell/Fe₃O₄:5/1). Therefore, the main and sharp peak attributed to the major phase of CaCO₃ in the structure of the eggshell.

Vibrating sample magnetometer analysis (VSM)

The vibrating sample magnetometer of Eggshell/Fe₃O₄ is illustrated in Figure 5. The magnetic behaviors of this nanocomposite were indicated by magnetic hysteresis. The super magnetic behavior of Fe₃O₄ nanoparticles was expected to be reduced after composition with

Eggshell. Nevertheless, the saturation magnetization of eggshell/Fe₃O₄ nanocomposite is 13 emu.g⁻¹ which shows the magnetic nature. Thus, the external magnetic field can easily separate the catalyst from the reaction mixture.

Synthesis of 4H-pyrans catalyzed by Eggshell/Fe₃O₄

The catalytic activity of nanocomposite was investigated in the 4H-pyrans synthesis. Therefore, to achieve the best conditions for the synthesis of 4H-pyrans, the three-component reaction of benzaldehyde, malononitrile, and ethyl acetoacetate was considered a model reaction. The results are summarized in Tables 3 and 4. To determine the best solvent for this reaction, different solvents were tested in the presence of 0.03 g Eggshell/Fe₃O₄ as a catalyst, and the best result was obtained with water and ethanol. We preferred to choose water as a solvent because it is the most eco-friendly solvent (Table 4). To obtain the optimized condition, various conditions were carried out for the reaction with ethyl acetoacetate (c), benzaldehyde (a), and malononitrile (b) (molar

ratio 1:1:1) as the model reaction (scheme1). The amount of ethyl 6-amino-5-cyano-2-methyl-4-phenyl-4H-pyran-3-carboxylate(d) was achieved with the lowest yields at room temperature (entries 1 and 2). In addition, increasing the temperature has affected on yield of the product. Furthermore, in (entries 3 and 4), the range of (60-80 °C) was considered the best result, and the middle effect on the quantitative yield of the desired product was obtained. Moreover, under solvent-free conditions, the yield has decreased, although the time reaction has not changed considerably. Our investigation has shown that the reflux condition has no considerable difference with EtOH or water. Therefore, water was defined as the best and green solvent in all derivatives of chromenes thoroughly (entries 7 and 8). It was amazing that using acetonitrile and dichloroethane as aprotic solvents in reflux conditions has not significantly affected yield and reaction time (entries 9 and 10). Finally, acetonitrile and dichloroethane solvents have produced lower yield reactions and higher reaction times than water and EtOH as protic solvents (entries 11 and 12).

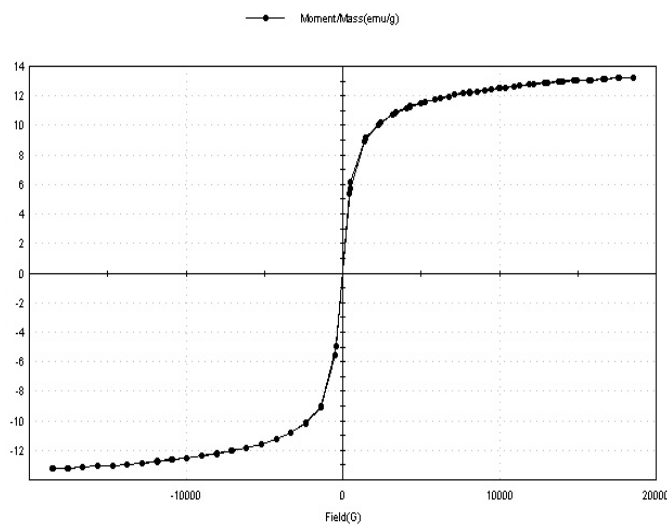


Figure 5. The VSM pattern of magnetic ES/Fe₃O₄

Table 3. Optimization of different amount of Eggshell/Fe₃O₄

Entry	Loading (mg)	Solvent	Temp. (°C)	Time (min)	Yield (%) ^a
1	0.01	H ₂ O	Reflux	180	42
2	0.02	H ₂ O	Reflux	120	53
3	0.03	H ₂ O	Reflux	10	96
4	0.04	H ₂ O	Reflux	10	95

^a Isolated yield**Table 4.** One pot three-component reaction of various aromatic aldehydes (a), malononitrile (b), and ethyl acetoacetate (c) via ES/Fe₃O₄ as a catalyst and water/reflux condition

Entry	Solvent	Temp. (°C)	Time (min)	Yield (%) ^a
1	H ₂ O	rt	270	40
2	EtOH	rt	270	40
3	H ₂ O	60	150	53
4	EtOH	60	150	53
5	-	60	180	47/3
6	-	80	180	49
7	Reflux	EtOH	10	96
8	Reflux	H ₂ O	10	96
9	Reflux	acetonitrile	200	60
10	Reflux	dichloroethane	120	50

^a Isolated yield

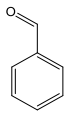
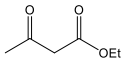
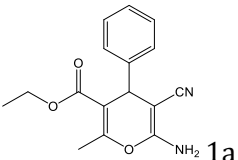
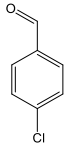
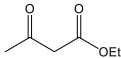
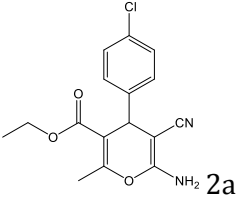
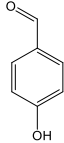
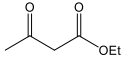
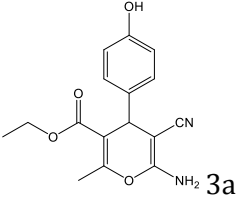
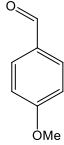
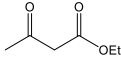
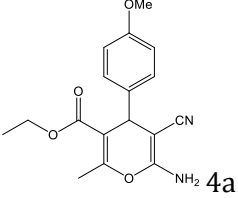
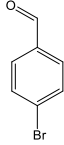
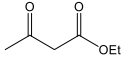
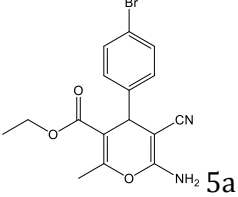
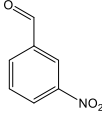
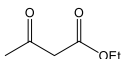
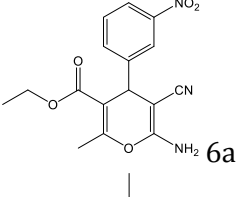
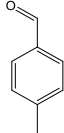
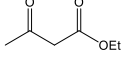
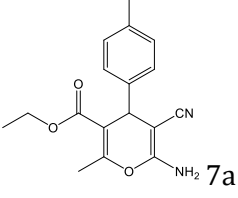
After optimization of the reaction conditions, to demonstrate the generality of this procedure, the synthesis was done with a wide range of aromatic aldehydes and hydroxyl/carbonyl compounds (Table 5).

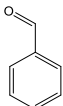
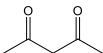
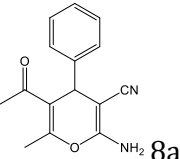
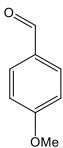
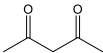
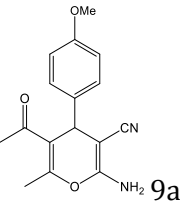
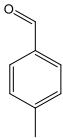
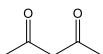
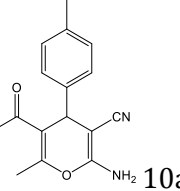
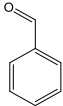
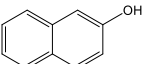
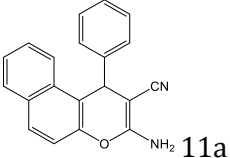
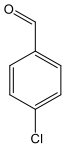
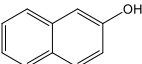
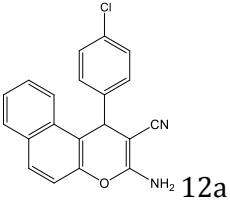
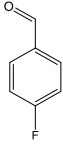
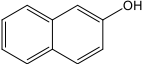
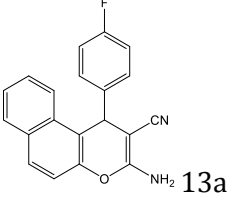
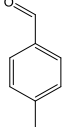
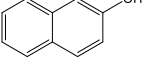
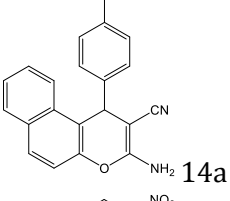
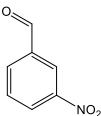
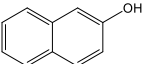
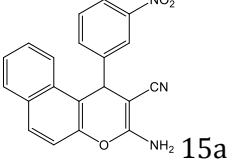
Interestingly, aromatic aldehydes with electron-withdrawing groups (Table 5, entries 2, 5, 6, 13, and 24), especially in 3 positions, took shorter to form the respective product compared with the electron-donating groups (Table 5, entries 3, 4, and 7). For more information, it could be the reason for substituted functional groups' intrinsic electronegativity induction effect. With the decrease of electron density in the aromatic ring, the electron-withdrawing groups cause convenient conditions to attack carbanion compounds.

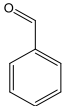
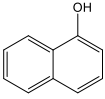
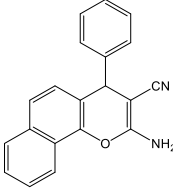
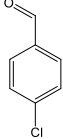
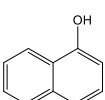
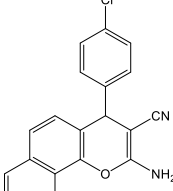
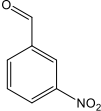
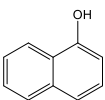
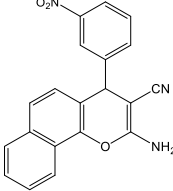
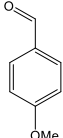
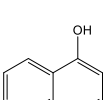
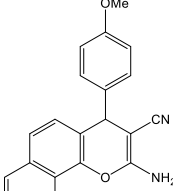
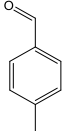
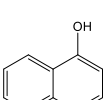
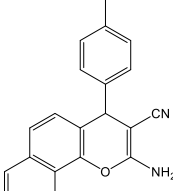
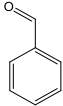
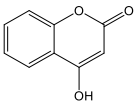
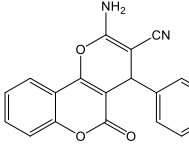
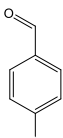
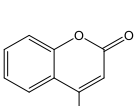
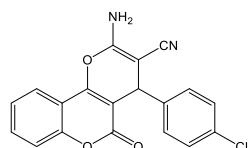
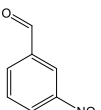
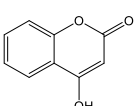
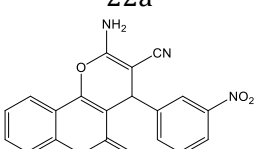
Different derivatives of 2-amino-5,10-dioxo-5,10-dihydro-4H-benzo[g]chromene were synthesized in a broad range of 1,3-di ketones

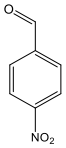
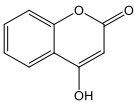
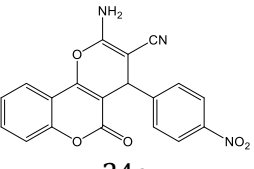
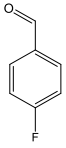
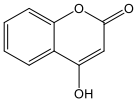
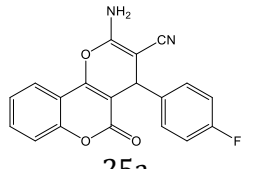
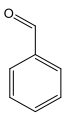
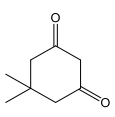
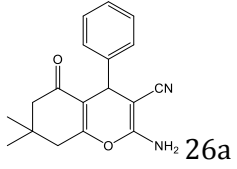
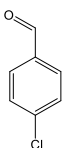
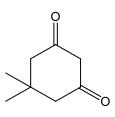
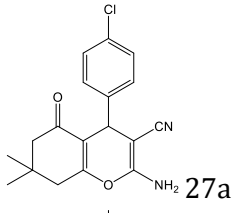
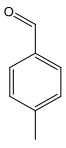
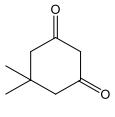
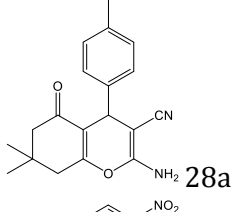
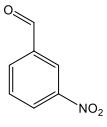
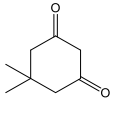
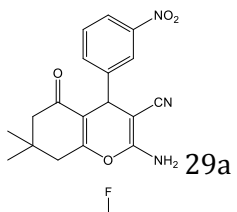
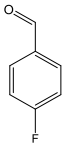
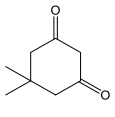
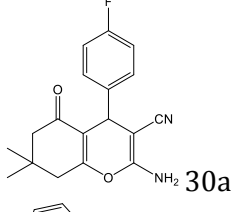
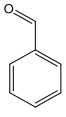
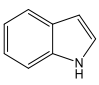
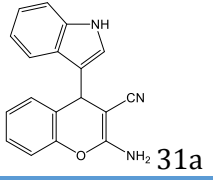
such as methyl acetoacetate, acetylacetone, 1-naphthol, 2-naphthol, dimedone, 4-hydroxycoumarin, indole, 4-chloro indol, and 4-methyl indol. In the presence of ethyl acetoacetate, the reaction time was lower than methyl acetoacetate and acetylacetone (Table 5, entries 1a-10a). After that, 1-naphthol and 2-naphthol were used as enolic components to synthesize 2-amino-4-phenyl-4H-benzo[h]chromene-3-carbonitrile (Table 5, entries 11a-20a). In this case, it was observed that the reaction time was lower than entries (Table 5, 1a-10a). The different stable resonance forms could cause it. Likewise, the production was produced in a shorter reaction time in the presence of 4-hydroxycoumarin than dimedone. As an enolic component (Table 5, entries 21a-30a). Indole and the last entries (Table 5, entries 31a-33a) showed the different electronegativity between oxygen and nitrogen.

Table 5. Synthesis of derivatives of 2-amino-5-oxo-5,6,7,8-tetrahydro-4H- benzo[b] pyran(4) via condensation of ethylacetoacetate, methylacetoacetate, acetylacetone, 1-naphtol, 2-naphtol, dimedone, 4-hydroxycoumarin, indol, 4-chloroindol, 4-methylindol (3), malononitrile (2), and in the presence of Eggshell/Fe₃O₄ as catalyst

Entry	Aldehydes (1)	Hydroxyl/carbonyl Compounds (3)	Product	Time(min)	Yield ^b (%)	M.p. Observed-[ref]
1				10	96	191-193 [34]
2				17	94	176-177 [35]
3				14	95	173-175 [36]
4				17	88	139-141 [37]
5				16	95	180-182 [38]
6				10	96	187-188 [39]
7				12	94	156-158 [40]

8				13	90	160-162 [41]
9				19	94	186-188 [42]
10				14	94	135-137 [43]
11				15	85	276-277 [44]
12				13	91	209-211 [45]
13				13	91	221-223 [46]
14				15	89	272-27 [47]
15				9	95	225-226 [44]

16				12	90	211-213 [48]
			16a			
17				10	91	232-233 [48]
			17a			
18				10	93	201-203 [36]
			18a			
19				15	88	181-183 [48]
			19a			
20				15	88	205-207 [49]
			20a			
21				10	90	259-261 [50]
			21a			
22				12	91	261-263 [51]
			22a			
23				9	95	263-265 [52]
			23a			

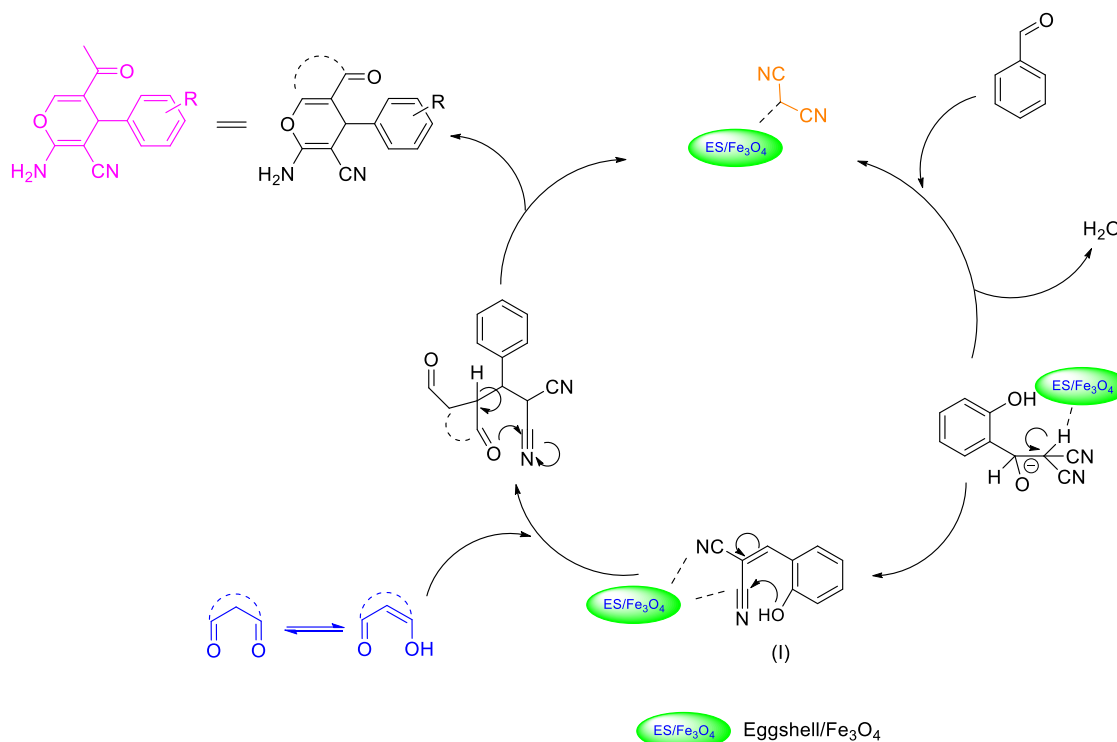
24				10	93	252-254 [53]
25				12	89	260-262 [37]
26				13	92	235-237 [54]
27				13	90	212-214 [55]
28				15	91	217-219 [56]
29				13	95	211-213 [57]
30				14	95	189-190 [58]
31				16	90	303-205 [59]

The suggested mechanism in [Scheme 3](#) has shown different steps of the one-pot three-component reaction. In the first step, a classical tandem sequence of Knoevenagel and Michael's

addition occurred. Acidic proton was released from malononitrile in the present alkali catalyst. The different aldehydes were tested in this reaction. A tandem Knoevenagel condensation-

cyclization reaction cause to form intermediate (I). The product was formed by tautomerization of the intermediate and the solvent has the main role in the three-component oriented synthesis of substituted 4*H*-pyrans, so the hydrogen bond persisted in both electrophile and nucleophile. Furthermore, the results have shown that the reaction conditions are different in all cases and

the effect of enolic component loading was screened. The reaction conveniently was done in water as a solvent and reflux condition and Eggshell/Fe₃O₄ (0/03 g) as the catalyst in the presence of 1-naphthol, 2-naphthol, Indole, dimedone, 4-hydroxycoumarin, 1,3-diketones such as (ethyl acetoacetate, acetylacetone, and methyl acetoacetate) as an enolic component.



Scheme 3. Reaction mechanism for the synthesis of tetra-substituted 4*H*-pyrans

Catalyst recovery and reusability

It is one of the most important advantages for industrial and commercial applications. When the reaction was completed, the mixture was filtered, and the recovered catalyst was washed with H₂O (5 mL) twice and reused after drying.

Conclusion

In the present study, for the first time, the synthesis of 2-amino-3-cyano-(4*H*)-chromene derivatives as an important class of organic

compounds, Eggshell/Fe₃O₄ as a new magnetic nanocomposite from natural source was used via green and eco-friendly conditions. The catalyst was characterized by Fourier Transform Infrared Spectroscopy (FT-IR), Scanning Electron Microscopy (SEM) and X-ray Diffraction (XRD), Thermal Gravimetric Analysis (TGA), and Vibrating Sample Magnetometer (VSM). The green and biodegradable catalyst, easy recovery, reusability of catalyst, and simple workup with quantitative yields are considerable advantages of this method. In all cases, the corresponding

functionalized 4H-pyrans were formed in high yield, the shortest reaction time, the easiest workup, no column-chromatography requirement, eco-friendly, and green catalyst. The Eggshell/Fe₃O₄ was reused several times without a substantially decreasing in yield percentages.

Acknowledgements

The authors gratefully acknowledge the partial support from the Research Council of the Iran University of Science and Technology.

Disclosure Statement

No potential conflict of interest was reported by the authors.

Funding

This research did not receive any specific grant from funding agencies in the public, commercial, or not-for-profit sectors.

Authors' Contributions

All authors contributed to data analysis, drafting, and revising of the paper and agreed to be responsible for all the aspects of this work.

Orcid

Hossein Ghafuri

<https://orcid.org/0000-0001-6778-985X>

Atefeh Emami

<https://orcid.org/0000-0002-0298-2154>

References

- [1]. Ding H., Zhou X.X., Zhang Z.H., Zhao Y.P., Wei J.S., Xiong H.M. *Nano Res.*, 2022, **15**:3548 [Crossref], [Google Scholar], [Publisher]
- [2]. Liu X., Zhou Y., Wang C.L., Liu Y., Tao D.J. *Chemical Engineering Journal*, 2022,

427:130878 [Crossref], [Google Scholar], [Publisher]

[3]. Ravanshad S., Asvar H., Fouladi F. *Asian J. Green Chem.*, 2020, **4**:173 [Crossref], [Publisher]

[4]. Pandya K.M., Dave B.P., Patel A.H. *Asian J. Green Chem.*, 2020, **4**:416 [Crossref], [Publisher]

[5]. Vikrant K., Kim K.H., Dong F., Boukhvalov D.W., Choi W. *Chemical Engineering Journal*, 2022, **428**:131177 [Crossref], [Google Scholar], [Publisher]

[6]. Attari A., Abbaszadeh-Mayvan A., and Taghizadeh-Alisaraie A. *Biomass Bioenergy*, 2022, **158**:106357 [Crossref], [Google Scholar], [Publisher]

[7]. Dianat M., Zare A., Hosainpour M. *Asian J. Nano. Mat.*, 2021, **4**:282 [Crossref], [Publisher]

[8]. Baghernejad B., Parhizgar S. *Asian J. Nano. Mat.*, 2021, **4**:178 [Crossref], [Publisher]

[9]. Ma P., Ding M., Liu X. *Chem. Eng. Sci.*, 2022, **252**:117530 [Crossref], [Google Scholar], [Publisher]

[10]. Chen M.M., Niu H.Y., Niu C.G. *J. Hazard. Mater.*, 2022, **424**:127196 [Crossref], [Google Scholar], [Publisher]

[11]. Nahar K. N., Rahaman M., Khan G. *Asian J. Green Chem.*, 2021, **5**:135 [Crossref], [Publisher]

[12]. Yadollahzadeh K. *Asian J. Nano. Mat.*, 2022, **5**:144 [Crossref], [Publisher]

[13]. Kiranakumar H.V., Thejas R., Naveen C.S., Ijaz Khan M., Prasanna G.D., Reddy S., Oreijah M., Guedri K., Bafakeeh O.T., Jameel M. *I. Biomass Convers. Biorefinery*, 2022 [Crossref], [Publisher]

[14]. Azlin M., Ilyas R., Zuhri M. *Polymers*, 2022, **14**:180 [Crossref], [Google Scholar], [Publisher]

[15]. Mohammadi R., Sabourmoghaddam N. *Asian J. Green Chem.*, 2020, **4**:11 [Crossref], [Publisher]

[16]. Mohammadi R., Sabourmoghaddam N. *Asian J. Green Chem.*, 2019, **4**:107 [Crossref], [Publisher]

- [17]. Oboudatian H.S., Safaei-Ghomi J. *Res Chem Intermed.*, 2022, **48**:2069 [[Crossref](#)], [[Google Scholar](#)], [[Publisher](#)]
- [18]. Chatterjee R., Bhukta S., Dandela R. J. *Heterocycl. Chem.*, 2022, **59**:633 [[Crossref](#)], [[Google Scholar](#)], [[Publisher](#)]
- [19]. Baghernejad B., Koosha S. *Journal of Applied Chemical Research*, 2020, **14**:19 [[Publisher](#)]
- [20]. S. Mowlazadeh, Haghighi A. P., Khalafi-Nezhad A., Oftadehgan S. *Asian J. Green Chem.*, 2022, **6**:203 [[Crossref](#)], [[Publisher](#)]
- [21]. Baghernejad B. and Fiuzat M. *Asian J. Nano. Mat.*, 2021, **4**:171 [[Crossref](#)], [[Publisher](#)]
- [22]. Rahmatpour F., Kosari M., Monadi N. *J. Mol. Struct.*, 2022, **1253**:132102 [[Crossref](#)], [[Google Scholar](#)], [[Publisher](#)]
- [23]. Nakhate A.V., Ingale A.P., Shinde S.V. *Polycycl. Aromat. Compd.*, 2022, **1** [[Crossref](#)], [[Google Scholar](#)], [[Publisher](#)]
- [24]. Korade S.N., Mhaldar P.M., Kulkarni P.P. *Synth. Commun.*, 2021, **51**:2336 [[Crossref](#)], [[Google Scholar](#)], [[Publisher](#)]
- [25]. Lati M.P., Shirini F., Alinia-Asli M. *J. Nanosci. Nanotechnol.*, 2020, **20**:973 [[Crossref](#)], [[Google Scholar](#)], [[Publisher](#)]
- [26]. Mansouri M., Habibi D., Heydari S. *Res. Chem. Intermed.*, 2022, **48**:683 [[Crossref](#)], [[Google Scholar](#)], [[Publisher](#)]
- [27]. Bita Baghernejad N.S.S. *Asian J. Green Chem.*, 2022, **6**:166 [[Crossref](#)], [[Publisher](#)]
- [28]. Baghernejad B. and Khoshnud Gilakejan S. *Asian J. Nano. Mat.*, 2022, **5**:1 [[Crossref](#)], [[Publisher](#)]
- [29]. Tashrifi Z., Mohammadi-Khanaposhtani M., Hamedifar H. *Mol. Divers.*, 2020, **24**:1385 [[Crossref](#)], [[Google Scholar](#)], [[Publisher](#)]
- [30]. Mamaghani M., Nia R.H., Tavakoli F. *Curr. Org. Chem.*, 2018, **22**:1704 [[Crossref](#)], [[Google Scholar](#)], [[Publisher](#)]
- [31]. Raj V., Lee J. *Front. Chem.*, 2020, **8**:623 [[Crossref](#)], [[Google Scholar](#)], [[Publisher](#)]
- [32]. Akbarpoor T., Khazaei A., Seyf J. Y. *Res. Chem. Intermed.*, 2020, **46**:1539 [[Crossref](#)], [[Google Scholar](#)], [[Publisher](#)]
- [33]. Mahmoudiani Gilan M., Khazaei A., Sarmasti N. *Res. Chem. Intermed.*, 2021, **47**:2173 [[Crossref](#)], [[Google Scholar](#)], [[Publisher](#)]
- [34]. Samir E.M., Mohareb R.M. *Bull. Chem. Soc. Ethiop.*, 2021, **35**:573 [[Crossref](#)], [[Google Scholar](#)], [[Publisher](#)]
- [35]. Hajlaoui A., Laajimi M., Znati M. *J. Mol. Struct.*, 2021, **1237**:130346 [[Crossref](#)], [[Google Scholar](#)], [[Publisher](#)]
- [36]. Malakooti R., Heravi M. M., Amiri Z. *Res. Chem. Intermed.*, 2022, **48**:3143 [[Crossref](#)], [[Google Scholar](#)], [[Publisher](#)]
- [37]. Thongni A., Phanrang P.T., Dutta A. *Synth. Commun.*, 2022, **52**:43 [[Crossref](#)], [[Google Scholar](#)], [[Publisher](#)]
- [38]. Tiwari J., Singh S., Saquib M. *Synth. Commun.*, 2018, **48**:188 [[Crossref](#)], [[Google Scholar](#)], [[Publisher](#)]
- [39]. Marak B.N., Hazarika B., Pandey S. K. *J. Mol. Struct.*, 2022, **133361** [[Crossref](#)], [[Google Scholar](#)], [[Publisher](#)]
- [40]. Azimzadeh-Sadeghi S., Yavari I. *J. Iran. Chem. Soc.*, 2021, **18**:1261 [[Crossref](#)], [[Google Scholar](#)], [[Publisher](#)]
- [41]. Khazaei A., Jahanshahi R., Sobhani S. *Green Chem.*, 2020, **22**:4604 [[Crossref](#)], [[Google Scholar](#)], [[Publisher](#)]
- [42]. Silambarasan S., Jamal Abdul Nasser A., Mohandas. *Acta Crystallographica Section E: Crystallographic Communications*, 2019, **75**:1568 [[Crossref](#)], [[Publisher](#)]
- [43]. Tamaddon F., Azadi D. *J. Iran. Chem. Soc.*, 2017, **14**:2077 [[Crossref](#)], [[Google Scholar](#)], [[Publisher](#)]
- [44]. Rezaei-Seresht E., Noroozi S., Mahdavi B. *Org. Prep. Proced. Int.*, 2022, **54**:268 [[Crossref](#)], [[Google Scholar](#)], [[Publisher](#)]
- [45]. Nabinia N., Shirini F., Tajik H. *J. Iran. Chem. Soc.*, 2018, **15**:2147 [[Crossref](#)], [[Google Scholar](#)], [[Publisher](#)]

- [46]. Zhu A., Li Q., Feng W. *Catal. Letters*, 2021, **151**:720 [[Crossref](#)], [[Google Scholar](#)], [[Publisher](#)]
- [47]. Azizi Amiri M., Pasha G.F., Tajbakhsh M. *Appl. Organomet. Chem.*, 2022, **36**:e6886 [[Crossref](#)], [[Google Scholar](#)], [[Publisher](#)]
- [48]. Mirza Aghayan M., Mohammadi M., Boukherroub R. *J. Heterocycl. Chem.*, 2022, **59**:1102 [[Crossref](#)], [[Google Scholar](#)], [[Publisher](#)]
- [49]. Patil S.P., Shinde S.K., Patil S.S. *Res. Chem. Intermed.*, 2022, **48**:5003 [[Crossref](#)], [[Google Scholar](#)], [[Publisher](#)]
- [50]. Kangani M., Hazeri N., Maghsoodlou M. T. *J. Chin. Chem. Soc.*, 2016, **63**:896 [[Crossref](#)], [[Google Scholar](#)], [[Publisher](#)]
- [51]. Keshavarz R., Farahi M., Karami B. *Acta Chim. Slov.*, 2021, **68**:332 [[Google Scholar](#)], [[Publisher](#)]
- [52]. Dekamin M. G., Eslami M., Maleki A. *Tetrahedron*, 2013, **69**:1074 [[Crossref](#)], [[Google Scholar](#)], [[Publisher](#)]
- [53]. Gholami R., Bamoniri A., Mirjalili B.B.F. *RSC Adv.*, 2022, **12**:27555 [[Crossref](#)], [[Google Scholar](#)], [[Publisher](#)]
- [54]. Chehab S., Merroun Y., Ghailane T. *J. Iran. Chem. Soc.*, 2021, **18**:2665 [[Crossref](#)], [[Google Scholar](#)], [[Publisher](#)]
- [55]. Taheri N., Fallah-Mehrzardi M., Sayyahi S. *Bull. Chem. Soc. Ethiop.*, 2018, **32**:531 [[Crossref](#)], [[Google Scholar](#)], [[Publisher](#)]
- [56]. Rahimzadeh G., Tajbakhsh M., Daraie M. *Appl. Organomet. Chem.*, 2022, **36**:e6829 [[Crossref](#)], [[Google Scholar](#)], [[Publisher](#)]
- [57]. Eivazzadeh Keihan R., Noruzi E. B., Radinekiyan F. *ChemistryOpen*, 2020, **9**:735 [[Crossref](#)], [[Google Scholar](#)], [[Publisher](#)]
- [58]. Khaleghi Abbasabadi M., Azarifar D., Esmaili Zand H.R. *Appl. Organomet. Chem.*, 2020, **34**:e6004 [[Crossref](#)], [[Google Scholar](#)], [[Publisher](#)]
- [59]. Baharfar R., Peiman S., Maleki B. *J. Heterocycl. Chem.*, 2021, **58**:1302 [[Crossref](#)], [[Google Scholar](#)], [[Publisher](#)]

How to cite this manuscript: Hossein Ghafuri*, Mahsan Zargari, Atefeh Emami . Green and eco-friendly synthesis of 2-amino-3-cyano-4H-chromene derivatives via Eggshell/Fe₃O₄ as a biodegradable polymer matrix nanocomposite. *Asian Journal of Green Chemistry*, 7(1), 2023, 54-69. DOI: 10.22034/ajgc.2023.1.7